PROCEEDINGS OF SPIE

SPIEDigitalLibrary.org/conference-proceedings-of-spie

Polarimetric and diffractive evaluation of 3.74 micron pixel-size LCoS in the telecommunications C-band

Mi Wang
Francisco J. Martínez
Andrés Márquez
Yabin Ye
Liangjia Zong
Inmaculada Pascual
Augusto Beléndez

SPIE.

Polarimetric and diffractive evaluation of 3.74 micron pixel-size LCoS in the telecommunications C-band

Mi Wang[1], Francisco J. Martínez[2,3], Andrés Márquez[2,3], Yabin Ye[1], Liangjia Zong[4], Inmaculada Pascual[2,5], Augusto Beléndez[2,3]

[1]ERC, Huawei Technologies Duesseldorf GmbH, Riesstrasse 25, D-80992 Munich, Germany
[2]Dept. de Física, Ing. de Sistemas y T. de la Señal, Univ. de Alicante, P.O. Box 99, E-03080, Alicante, Spain
[3]I.U. Física Aplicada a las Ciencias y las Tecnologías U. de Alicante, P.O. Box 99, E-03080, Alicante, Spain
[4]Huawei Technologies Co., Ltd., Bantian, Longgang District, Shenzhen 518129, P. R. China
[5]Dept. de Óptica, Farmacología y Anatomía, Universidad de Alicante, P.O. Box 99, E-03080, Alicante, Spain

ABSTRACT

Liquid-crystal on Silicon (LCoS) microdisplays are one of the competing technologies to implement wavelength selective switches (WSS) for optical telecommunications. Last generation LCoS, with more than 4 megapixels, have decreased pixel size to values smaller than 4 microns, what increases interpixel cross-talk effects such as fringing-field. We proceed with an experimental evaluation of a 3.74 micron pixel size parallel-aligned LCoS (PA-LCoS) device. At 1550 nm, for the first time we use time-average Stokes polarimetry to measure the retardance and its flicker magnitude as a function of voltage. We also verify the effect of the antireflection coating when we try to characterize the PA-LCoS out of the designed interval for the AR coating. Some preliminary results for the performance for binary gratings are also given, where the decrease of modulation range with the increase in spatial frequency is shown, together with some residual polarization effects.

Keywords: Liquid-crystal devices, Parallel-aligned, Birefringence, Spatial light modulators, wavelength selective switch (WSS), optical interconnects, crosstalk.

1. INTRODUCTION

Liquid-crystal on Silicon (LCoS) microdisplays[1] is one of the most widespread technologies used nowadays for spatial light modulation applications. Among them, parallel-aligned LCoS (PA-LCoS) are especially interesting since they enable phase-only operation without coupled amplitude modulation[2][3][4], what is interesting for a wide range of optics and photonics applications, such as in diffractive optics[5], optical storage[6][7], optical metrology[8], reconfigurable interconnects[9][10], wavefront sensing of structured light beams[11], holographic optical traps[12], or quantum optical computing[13].

In particular LCoS microdisplays are one of the competing technologies to implement reconfigurable optical interconnects and more specifically wavelength selective switches (WSS) for optical telecommunications[14][15][16][17]. These systems are the current promising solution for further increasing the traffic capacity in fiber networks. In order to increase the spatial bandwidth and resolution, last generation LCoS have decreased pixel size to values smaller than 4 microns, while increasing the number of pixel elements to more than 4 megapixels. This increases the port count number, thus enabling a superior manageable interconnection capacity bandwidth. However, for the LCoS to be applied in the telecommunication C-band (1.55 micron wavelength) the liquid-crystal layer needs to be significantly thicker than when used in the visible spectrum. The large ratio between the thickness with respect to the pixel size introduces important vicinity problems between neighbouring pixels due to the fringing-field and other cross-talk related phenomena[18][19][20][21].

In the present work we proceed with an experimental evaluation of a 3.74 micron pixel size parallel-aligned LCoS (PA-LCoS) device. We evaluate its performance with well-established techniques already applied to larger pixel size PA-LCoS microdisplays in the visible[22]. We analyse with time-average Stokes polarimetry the retardance and its flicker magnitude as a function of voltage[23]. Flicker is a typical degradation effect in modern LCoS devices, especially in the digitally addressed[24][25][26][27]. These techniques had been applied to previous PA-LCoS in the visible as polarization

Optics and Photonics for Information Processing XI, edited by Khan M. Iftekharuddin, Abdul A. S. Awwal, Mireya García Vázquez, Andrés Marquez, Víctor Diaz-Ramirez, Proc. of SPIE Vol. 10395, 103951J · © 2017 SPIE · CCC code: 0277-786X/17/$18 · doi: 10.1117/12.2277451

conversors[28], to display multilevel diffractive optical elements[29] and in holographic data storage systems[30]. In this work we demonstrate the applicability of these techniques to the telecommunications C-band illumination and to this novel smaller pixel size PA-LCoS devices. We also take a qualitative look at the existence of residual or induced twist of the LC director: small deviations in some of the experimental results can be interpreted as due to small twist between the entrance and backmirror faces. We also provide some preliminary results dealing with the display of binary gratings of various periodicities and orientations. Our analysis is based on the polarimetric analysis of the transmitted order, i.e. zero diffracted. This polarimetric analysis is useful to provide a more thorough characterization of the performance of the PA-LCoS. In particular, it shows to which degree the cross-talk effects between pixels, such as fringing-field, generate a performance which is largely dependent on the spatial frequency of the element addressed onto the microdisplay.

2. TIME-AVERAGED STOKES POLARIMETRY

Time-averaged Stokes polarimetry to characterize the average retardance and its flicker was first proposed and demonstrated in the visible[23] for the PLUTO device, a PA-LCoS with a pixel pitch of 8 μm. Here we provide a brief explanation of this theoretical approach, which is composed of both a model for the time evolution of the retardance fluctuations in PA-LC devices, and reverse-engineering calibration procedure to extract the value of the parameters in the model. The phase flicker exhibited by LCoS devices within the frame period has been found to be properly approximated by a triangular time-dependent profile[23][31]. If we consider the averaged value for a measurement integration time equal or larger than the addressing frame period what we get is that the state of polarization (SOP) for the light beam reflected by the LCoS may not be fully polarized. This leads us to use the Mueller-Stokes formalism, which enables to deal both with polarized and unpolarized light[32], to describe the action of PA-LCoS displays on the light beam. Applying this formalism and taking into account the triangular time-dependent profile for the linear retardance, we obtained the following matrix for a linear variable retarder with flicker,

$$\left\langle M_R(\overline{\Gamma},a)\right\rangle = \begin{pmatrix} 1 & 0 & 0 & 0 \\ 0 & 1 & 0 & 0 \\ 0 & 0 & (\sin a/a)\cos\overline{\Gamma} & (\sin a/a)\sin\overline{\Gamma} \\ 0 & 0 & -(\sin a/a)\sin\overline{\Gamma} & (\sin a/a)\cos\overline{\Gamma} \end{pmatrix} \tag{1}$$

, where $\overline{\Gamma}$ is the average retardance within the frame period and a its fluctuation amplitude, defined as half the maximum-to-minimum value for the fluctuation. To calibrate the values for these two parameters in the model we measured the averaged Stokes vector parameters for an input light beam linearly polarized light at +45º with respect to the X axis, i.e. (S0=1, S1=0, S2=1, S3=0). The analytical expressions for the reflected averaged Stokes vector and for the degree of polarization (DOP) are very simple in this case,

$$\left\langle S_{out}\right\rangle = \begin{pmatrix} 1 \\ 0 \\ -(\sin a/a)\cos\overline{\Gamma} \\ (\sin a/a)\sin\overline{\Gamma} \end{pmatrix} \tag{2}$$

$$DoP = (\sin a/a) \tag{3}$$

Eventually, the calibration can be easily accomplished using Eq. (3) to obtain the fluctuation amplitude a, and the ratio between the 3rd and 4th Stokes vector components, i.e. $-\langle S_3\rangle/\langle S_2\rangle = tg(\overline{\Gamma})$, to obtain $\overline{\Gamma}$ [23].

3. RETARDANCE AND FLICKER AMPLITUDE IN THE C-BAND

3.1 Characterization

The PA-LC device that we consider in the present work is a commercial PA-LCoS display, model GAEA distributed by the company HOLOEYE. It is filled with a nematic liquid crystal, with 3840x2160 pixels and 0.7" diagonal, 3.74 µm pixel pitch, 90% fill factor, and digitally addressed, at 30 Hz. By means of a USB interface and its correspondingly provided software, we can configure the modulator for different applications and wavelengths. Besides, as with the larger pixel size PLUTO devices[33], different pulse width modulation (PWM) addressing schemes (digital addressing sequences) can be generated by the driver electronics[24][33]. The low and high voltage levels for the binary signal applied across the LC layer can be configured using the software of the device, as it was the case with the PLUTO device[33]. In the GAEA device these low and high voltages are called "Black1" and "White1" respectively. Altogether, in the present work we consider the digital addressing sequence "6-5", consisting of 6 "equally weighted" bit planes and 5 "binary" bit planes[33]. In particular we consider the configuration file "6-5_1550nm_2pi_linear" that comes with the software and that includes the digital addressing sequence, the gamma table, and default values for the Black1 and White1 voltages, which are 0.563 V and 1.572 V. Due to the actual gamma curve implemented, the actual number of quantization levels for this configuration is limited to 174, out of the maximum of 224 possible levels for the sequence 6-5. We note that the GAEA device embeds a temperature sensor whose value is displayed in the software controlling the device. There is the possibility to mount the panel onto a heatsink. We checked that with the heatsink the temperature delivered is about 38ºC and without is about 50º. The measurements in the paper are without the heatsink. No big difference was found, mainly a slightly smaller flicker amplitude with the heatsink.

In Fig 1 we show the experimental setup for retardance and flicker measurement. The LC director for the GAEA device is parallel to the long axis of its aperture, which is along the horizontal of the lab. Illumination wavelength is 1550 nm from a continuous wave laser, model OE4020 from OEwaves. Linearly polarized light vibrating at +45º with respect to the vertical of the lab, which is the X-axis of our reference system, impinges almost perpendicularly onto the entrance window of the device. We note that alignment of the beam direction with the entrance cavity of the polarimeter is very tricky in the infrared since we cannot see the direction of the input light with the naked eye and we need to use auxiliary elements like infrared cards. For a better control, we mounted the polarimeter onto a tip-tilt platform and we combined two translation stages for transversal and vertical repositioning.

Different gray levels are addressed to the display and the SOP of the reflected light is measured with a Stokes polarimeter (model PAX5710IR2-T from THORLABS), which provides the time-averaged Stokes parameters for an interval of 600 ms, much longer than the characteristic flicker period (in the order of a few milliseconds). The working geometry considered in this paper corresponds to quasi-perpendicular incidence[22] (actual angle of incidence is smaller than 3º). We note that the director axis (extraordinary axis) in nematic based LCoS generally corresponds to the slow axis. In the present LCoS the director axis is along the horizontal of the laboratory reference system.

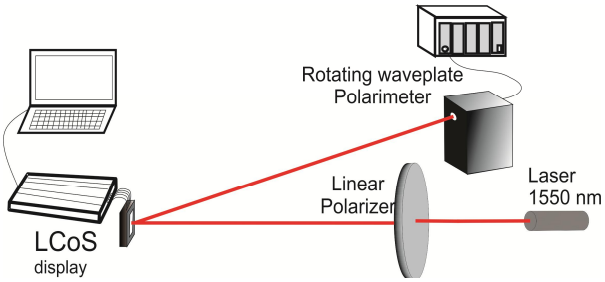

Fig. 1. Schematic of the experimental setup for Time-Averaged Stokes Polarimetry.

In Fig. 2 we show in four plots the results for the averaged output SOP measured with the polarimeter by applying the time-averaged Stokes polarimetry technique. We show both the measurements as a function of voltage and as a reference we also show the measurement when the LCoS is switched off (off-state value indicated in the legends). We show the power normalized by its maximum value, i.e. normalized S_0 Stokes parameter, and the degree of polarization, DOP, in plot (a). DOP is almost one along the whole gray level range, and power exhibits some small fluctuation with the gray level, that could be light that is being redistributed between the pixilation orders of the GAEA device: even though we

are addressing uniform screens, since it is a pixelated device there are diffraction orders, and our measurements correspond to the zero order of the pixelation. In plot (b) we shown the normalized Stokes parameters S_1, S_2 and S_3, where we see the oscillations in the two latter, whereas S_1 is almost zero for the whole gray level range, as given by Eq. (2). From the normalized Stokes parameters, the azimuth (plot (c)) and ellipticity (plot (d)) of the output SOP can be obtained, which is sometimes more intuitive. We see that output light is changing ellipticity linearly with the gray level, with the axis of the ellipse along the axes of the input polarizer at ±45º with respect to the vertical of the lab (X-axis).

In Fig. 3 (a) and (b) we show respectively the calibrated values for the average retardance and its flicker amplitude versus the gray level addressed (voltage), and also for the off-state values. We observe that the retardance range is about 360º with a very good linearity. We see that the off-state value does not coincide with the one at zero gray level, indicating that there is already a voltage applied. The fluctuation amplitude reaches 10º, which is a very small value as discussed in previous papers[22][23][29]. We note that for DoP>1, non-physical values, we consider that fluctuation amplitude is 0º, as can be seen at a few gray levels. We also see some discrete jumps in the flicker, which are due to the pulsed nature of the digital signal addressed onto the LCoS[23].

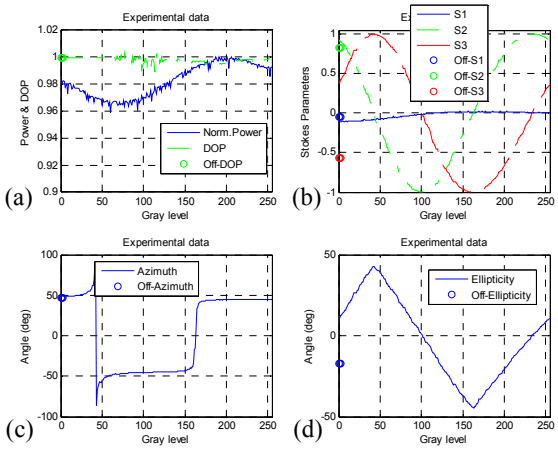

Fig. 2. Output SOP measured with the polarimeter for linearly polarized light at 45º. Both on-state and off-state measurements are given for the various parameters, as indicated in the legends. (a) DOP and normalized output Power, (b) Stokes parameters, (c) Azimuth, (d) Ellipticity. For the configuration "6-5_1550nm_2pi_linear" with (Black1, White1) = (0.563V, 1.572V), for λ=1550 nm, and for quasi-perpendicular incidence at 3º.

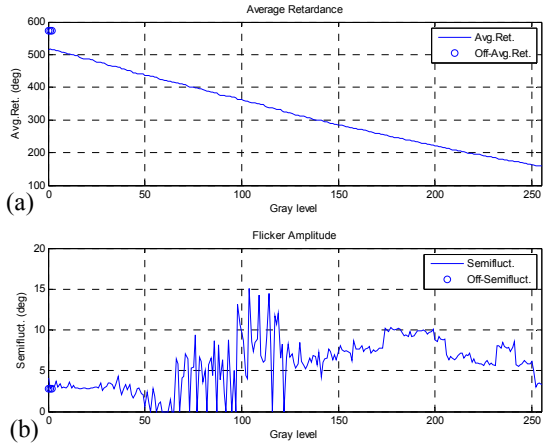

Fig. 3. Calculated values, both on-state and off-state, for (a) average retardance and (b) fluctuation amplitude. For the configuration "6-5_1550nm_2pi_linear" with (Black1, White1) = (0.563V ,1.572V), for λ=1550 nm, and for quasi-perpendicular incidence at 3º.

3.2 Predictive capability

Next, we check if the previous calibration and the time-averaged Stokes polarimetry technique is actually valid for the GAEA device and for the infrared telecommunications C-band. We compare experimental results obtained for other input SOPs and the calculated values using the average retardance and the flicker in Fig. 3. In Fig. 4 we show this comparison for input SOP linearly polarized at 20º with respect to the vertical of the lab (plots (a1) and (b1)), and for input SOP right-handed circular (RHC) (plots (a2) and (b2)). Plots (a1) and (a2) correspond to the DOP, and plots (b1) and (b2) correspond to the normalized Stokes parameters S_1, S_2 and S_3. We can clearly see the excellent agreement between model and experiment. It is especially noticeable that we can predict the DOP for RHC with such a good accuracy since its variation is very small, then we can say that the technique is very accurate and sensitive. In the case of the DOP for linearly polarized light at 20º, we note that the experimental DOP is slightly larger than 1, within the range of accuracy of the polarimeter: prediction has the same shape but with a slight offset.

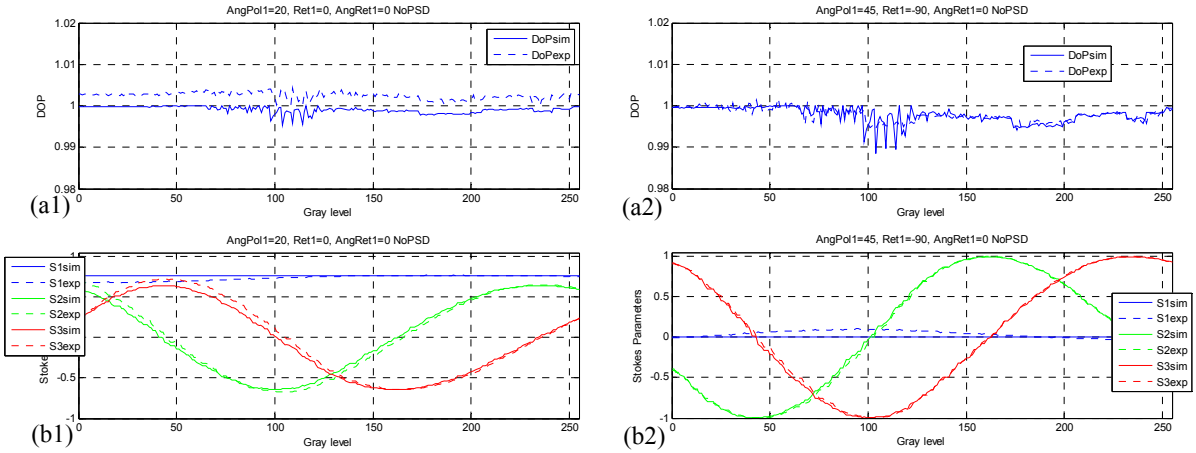

Fig. 4. Comparison between experimental and calculated values for the DOP and normalized Stokes parameters for input SOP: (a1) and (b1) for linearly polarized light at 20º, (a2) and (b2) for right-handed circular. For the configuration "6-5_1550nm_2pi_linear" with (Black1, White1) = (0.563V ,1.572V), for λ=1550 nm, and quasi-perpendicular incidence at 3º.

4. EFFECT OF THE ANTIREFLECTION COATING IN THE VISIBLE

The GAEA device we have in the lab is the one sold by Holoeye for telecom applications. In principle, it has an antireflection (AR) coating assuring a front reflection of less than 0.5% between 1400 and 1700 nm[34]. We want to check what happens when we leave this interval and illuminate in the visible range. In principle, at shorter wavelengths the retardance range increases and there are applications where having ranges much larger than 2π radians is interesting as in the case of multiorder diffractive optical elements[35]. To this goal we illuminate with a He-Ne laser at 633 nm and we substitute the optical head of the polarimeter for the corresponding to the visible spectrum (PAX5710VIS-T). We note that other elements in the setup, such as polarizers and retarders, need to be replaced as well for the ones appropriate for the visible spectrum.

In Fig. 5 we show the results for the output SOP for an input state linearly polarized at +45º from the vertical of the lab, as it was the case in Fig. 2. The four plots composing Fig. 5 are analogous to the ones in Fig. 2. We clearly see that the results obtained show a very different behavior when compared with the ones in Fig. 2. For example, in Fig. 5(b) we see that the Stokes parameters S_2 and S_3 do not follow the oscillation behavior, which is associated with a linear retarder, found in Fig. 2(b). In addition, S_1 is clearly different from zero, in contrast with Eq. (2). Probably the existence multiple interferences between the multiple reflections originated at 633 nm are producing this behavior. In conclusion, out of the AR coating interval the GAEA device is not behaving as a linear retarder and the characterization of its performance cannot be modeled just with the average retardance and the flicker amplitude parameters. Probably the AR coating for

the infrared is enhancing the existence of multiple interferences in the visible, thus making the device not useful for applications.

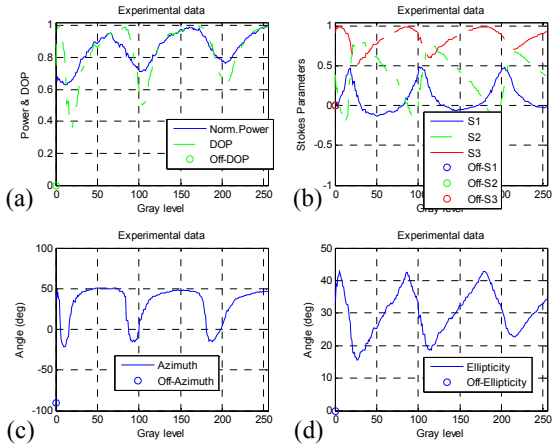

Fig. 5. Output time-averaged SOP measured with the polarimeter for linearly polarized light at 45º. Both on-state and off-state measurements are given for the various parameters, as indicated in the legends. (a) DOP and normalized output Power, (b) Stokes parameters, (c) Azimuth, (d) Ellipticity. For the configuration "6-5_1550nm_2pi_linear" with (Black1, White1) = (0.563V, 1.572V), for λ=633 nm, and for quasi-perpendicular incidence at 3º.

5. BINARY GRATINGS: ZERO-ORDER POWER AND STATE OF POLARIZATION

In previous Sections we have shown characterization of the GAEA when addressing uniform gray level screens. The ultimate application where we are interested for the GAEA is to implement reconfigurable optical interconnects and more specifically wavelength selective switches (WSS) for optical telecommunications. This usually corresponds to periodic optical elements, such as blazed gratings[5] which steer the beam into a specific deflection angle as a function of the period. The shorter the period the larger the deflection angle. The uniform screen is equivalent to the limiting case of an infinite period grating.

To analyse what is the effect of finite period on the modulation characteristics of the GAEA device we will address binary gratings of different periodicities, in the range from 2 to 20 pixels per period. We will consider horizontal and vertical gratings, i.e. periodicity is respectively in rows/period and columns/period. We note that in previous LCD[36] and LCoS[37] devices it has been found that their modulation range shortens for shorter periods, and also shortens for vertical gratings. This has been named as the anamorphic and frequency dependent effect[36][37]. The causes may be various, but in principle two of the most important are the appearance of tangential components in the applied electric field, i.e. fringing-field, and vicinity LC adherence effects[18][19][20][21]. This interpixel cross-talk effects limit the appearance of sharp boundaries, thus they produce a low-pass filtering of the image addressed to the display.

In our experiment we illuminate the GAEA device with linearly polarized light parallel to the LC-director, i.e. polarized along the horizontal of the lab. Then, the PA-LCoS works as a phase-only spatial light modulator, and ideally the SOP for the light reflected must also be linearly polarized along the horizontal. At the output of the PA-LCoS we will now obtain various diffraction orders produced by the binary grating, where we address a fix 0 gray level to one semiperiod and a variable gray level to the other semiperiod. We will measure the average Stokes vector for the zero-diffracted order, whose direction is always the same independently of the period for the binary grating. This makes it easy for the Stokes polarimeter to be used to analyse its state of polarization, thus providing a large amount of information.

In Fig. 6 we show the time-averaged SOP for the zero-order when addressing binary gratings of period 2 and 20 pixels (see legends), which is the minimum and maximum periods that we are addressing. In plots (a1), (b1), (c1) and (d1) for horizontal gratings, and it plots (a2), (b2), (c2) and (d2) for vertical gratings. We note that the sequence of plots for analysis of results for the output SOP is equivalent to the sequence of plots in Fig. 2 and Fig. 5: (a) DOP and normalized output power, (b) Stokes parameters, (c) Azimuth, and (d) Ellipticity.

In plots 6 (a1) and (a2) we see that the power in the zero-order varies very differently for the period 2, with no minimum, and 20, where it reaches a minimum and then increases to a value about 0.6. In principle, for a binary phase grating, when the phase step is 180º then a null is obtained and when it is 360º a maximum in the zero-order is obtained since it is not distinguishable from a uniform gray level screen. According to the calibration in Fig. 2, the phase step is 180º at about gray level 120, indicated by the red dash vertical line, and it is 360º at about gray level 255. We see that for period 20 the minimum approaches the red dash line even though it happens at slightly larger gray levels. At 255 gray level we see that for period 20 the intensity is clearly smaller than one, which indicates that the grating has smoothen its profile and/or the phase step is smaller than 360º. For the case of period 2 is even more evident the deviations with respect to the calibration performed for uniform screens in Fig. 2. When comparing the power for horizontal (a1) and vertical (a2) gratings we see that evolution for vertical gratings is slightly slower than for horizontal, thus cross-talk effects are a bit more relevant, even though the difference is very small. If we now take a look at DOP we see that it is about one except for grating with period 20 about the area with the minimum, where there is no energy, so the smaller DOP could be simply produced by the lack of signal.

Let us know discuss the SOP information in plots (b1) and (b2). In the case of the grating with period 2 we observe some small deviation from the case of linearly polarized light along the horizontal. This is more evident in plots (d1) and (d2) where the ellipticity becomes slightly different from 0º. In the case of period 20 we observe that deviations appear in the proximity of the intensity minimum. Since deviations are small, the appearance of residual polarization effects because of the above mentioned interpixel cross-talk phenomena needs a more careful analysis.

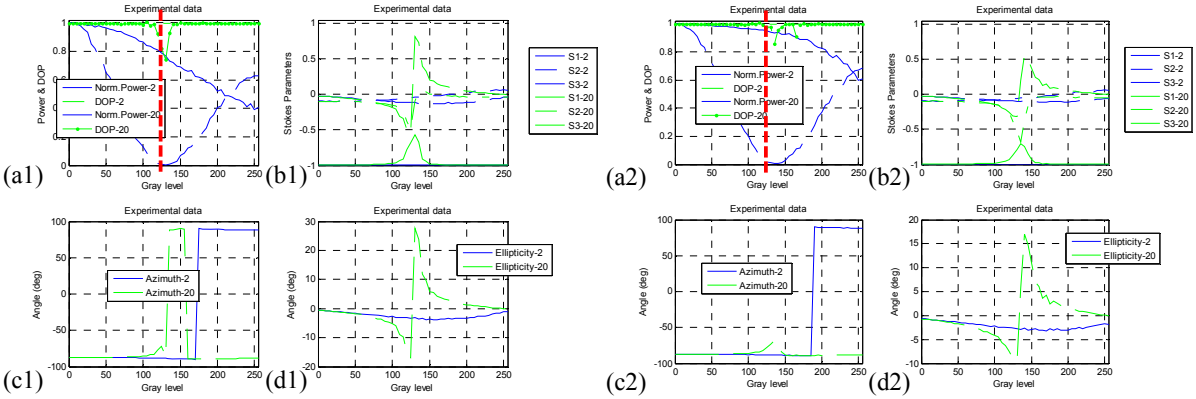

Fig. 6. Output time-averaged SOP at the zero-order for the binary phase gratings with period 2 and 20, measured with the polarimeter. (a1) and (a2) DOP and normalized output Power, (b1) and (b2) Stokes parameters, (c1) and (c2) Azimuth, (d1) and (d2) Ellipticity. (a1), (b1), (c1) and (d1) for horizontal gratings, and (a2), (b2), (c2) and (d2) for vertical gratings. For the configuration "6-5_1550nm_2pi_linear" with (Black1, White1) = (0.563V, 1.572V), for λ=1550 nm, and for quasi-perpendicular incidence at 3º. Input light linearly polarized along the horizontal, and no analyzer.

6. CONCLUSIONS

In this work we have demonstrated that time-averaged Stokes polarimetry is an accurate technique enabling to measure the average retardance and the flicker amplitude at 1550 nm in a PA-LCoS with pixel smaller than 4 μm, as it is the case of the GAEA device. This calibration is performed for uniform screens. A detailed analysis is done afterwards to characterize the cross-talk effects when spatial frequencies are addressed. We analyze the DOP, diffracted power and SOP for the zero-order of binary gratings with different periodicities and for vertical and horizontal orientations. We clearly obtain that cross-talk effects in the power increase with the decrease in the period, and they are slightly stronger for vertical gratings. With respect to polarization effects due to cross-talk, they exist but are very small, thus a more careful analysis is necessary to extract a more definite conclusion. We also verify the effect of the antireflection coating when we try to characterize the PA-LCoS out of the designed interval for the antireflection coating. We see that the multiple interferences that arise make that the PA-LCoS is not behaving as a linear retarder, then it cannot be used properly outside of the infrared C-band.

ACKNOWLEDGEMENTS

Work supported by Ministerio de Economía, Industria y Competitividad (Spain) (FIS2014-56100-C2-1-P and FIS2015-66570-P) and by Generalitat Valenciana (Spain) (PROMETEO II/2015/015). This work has been supported by the EC through H2020 project ROAM (Grant no: 645361 www.roam-project.eu).

REFERENCES

[1] S. T.Wu, D. K. Yang. [Reflective Liquid Crystal Displays], John Wiley & Sons Inc. (2005).
[2] N. Collings, T. Davey, J. Christmas, D. Chu, and B. Crossland, "The Applications and Technology of Phase-Only Liquid Crystal on Silicon Devices," J. Display Technol. 7, 112-119 (2011).
[3] G. Lazarev, A. Hermerschmidt, S. Krüger, and S. Osten, "LCOS Spatial Light Modulators: Trends and Applications," in [Optical Imaging and Metrology: Advanced Technologies], W. Osten and N. Reingand, eds., John Wiley & Sons (2012).
[4] Z. Zhang, Z. You, and D. Chu, "Fundamentals of phase-only liquid crystal on silicon (LCOS) devices," Light Sci. Appl. 3, 1-10 (2014).
[5] J. Turunen and F. Wyrowski, eds., [Diffractive Optics for Industrial and Commercial Applications], Akademie Verlag (1997).
[6] H. J. Coufal, D. Psaltis, and B. T. Sincerbox, eds., [Holographic Data Storage], Springer-Verlag (2000).
[7] K. Curtis, L. Dhar, A. Hill, W. Wilson, and M. Ayres, eds., [Holographic Data Storage: From Theory to Practical Systems], John Wiley & Sons, Ltd, (2010).
[8] W. Osten, C. Kohler, and J. Liesener, "Evaluation and application of spatial light modulators for optical metrology," Opt. Pura Apl. 38, 71-81 (2005).
[9] M. A. F. Roelens, S. Frisken, J. A. Bolger, D. Abakoumov, G. Baxter, S. Poole, and B. J. Eggleton, "Dispersion trimming in a reconfigurable wavelength selective switch," J. Lightw. Technol. 26, 73–78 (2008).
[10] M. Salsi, C. Koebele, D. Sperti, P. Tran, H. Mardoyan, P. Brindel, S. Bigo, A. Boutin, F. Verluise, P. Sillard, M. Bigot-Astruc, L. Provost, and G. Charlet, "Mode-Division Multiplexing of 2 100 Gb/s Channels Using an LCOS-Based Spatial Modulator," J. Lightwave Technol. 30, 618–623 (2012).
[11] A. Dudley, G. Milione, R. R. Alfano, and A. Forbes, "All-digital wavefront sensing for structured light beams," Opt. Express 22, 14032-14040 (2014).
[12] A. Farré, M. Shayegan, C. López-Quesada, G. A. Blab, M. Montes-Usategui, N. R. Forde, E. Martín-Badosa, "Positional stability of holographic optical traps," Opt. Express 19, 21370-21384 (2011).
[13] M. A. Solís-Prosser, A. Arias, J. J. M. Varga, L. Rebón, S. Ledesma, C. Iemmi, and L. Neves, "Preparing arbitrary pure states of spatial qudits with a single phase-only spatial light modulator," Opt. Lett. 38, 4762-4765 (2013).
[14] T. A. Strasser and J. L. Wagener, "Wavelength-Selective Switches for ROADM Applications," IEEE Journal of Selected Topics in Quantum Electronics 16(5), 1150-1157 (2010).
[15] S. Frisken, G. Baxter, D. Abakoumov, H. Zhou, I. Clarke, S. Poole, "Flexible and grid-less wavelength selective switch using LCOS technology," Proc. Optical Fiber Communication Conference and Exposition (OFC/NFOEC), 1-3 (2011).
[16] J. He, R. A. Norwood, M. Brandt-Pearce, I. B. Djordjevic, M. Cvijetic, S. Subramaniam, R. Himmelhuber, C. Reynolds, P. Blanche, B. A. Lynn, "A survey on recent advances in optical communications," Comput. Elect. Eng. 40 (1), 216-240 (2014).
[17] M. Wang, L. Zong, L. Mao, A. Marquez, Y. Ye, H. Zhao, F. J. Vaquero, "LCoS SLM Study and Its Application in Wavelength Selective Switch," Photonics 4(22), 1-16 (2017).
[18] B. Apter, U. Efron, and E. Bahat-Treidel, "On the fringing-field effect in liquid-crystal beam-steering devices," Appl. Opt. 43, 11–19 (2004).
[19] E. Hällstig, J. Stigwall, T. Martin, L. Sjöqvist, M. Lindgren, "Fringing fields in a liquid crystal spatial light modulator for beam steering," J. Mod. Opt. 51 (8), 1233-1247 (2004).
[20] X. Wang, B. Wang, P. J. Bos, P. F. McManamon, J. J. Pouch, F. A. Miranda, J. E. Anderson, "Modeling and design of an optimized liquid-crystal optical phased array," J. Appl. Phys. 98(7), 073101 (2005).

[21] C. Lingel, T. Haist, and W. Osten, "Optimizing the diffraction efficiency of SLM-based holography with respect to the fringing field effect," Appl. Opt. 52, 6877–6883 (2013).
[22] F.J. Martínez, A. Márquez, S. Gallego, M. Ortuño, J. Francés, A. Beléndez, and I. Pascual, "Averaged Stokes polarimetry applied to evaluate retardance and flicker in PA-LCoS devices," Opt. Express 22, 15064-15074 (2014).
[23] F.J. Martínez, A. Márquez, S. Gallego, J. Francés, I. Pascual, and A. Beléndez, "Retardance and flicker modeling and characterization of electro-optic linear retarders by averaged Stokes polarimetry," Opt. Lett. 39, 1011-1014 (2014).
[24] A. Hermerschmidt, S. Osten, S. Krüger, and Thomas Blümel, "Wave front generation using a phase-only modulating liquid-crystal based micro-display with HDTV resolution," Proc. SPIE 6584, 65840E (2007).
[25] A. Lizana, I. Moreno, A. Márquez, E. Also, C. Iemmi, J. Campos, and M.J.Yzuel, "Influence of the temporal fluctuations phenomena on the ECB LCoS performance," Proc. SPIE 7442, 74420G-1 (2009).
[26] J. García-Márquez, V. López, A. González-Vega, and E. Noé, "Flicker minimization in an LCoS spatial light Modulator," Opt. Express 20, 8431-8441 (2012).
[27] F. J. Martínez, A. Márquez, S. Gallego, J. Francés, and I. Pascual, "Extended linear polarimeter to measure retardance and flicker: application to LCoS devices in two working geometries," Opt. Eng. 53, 014105 (2014).
[28] A. Márquez, F. J. Martínez, S. Gallego, M. Ortuño, J. Francés, A. Beléndez, and I. Pascual, "Averaged Stokes polarimetry applied to characterize parallel-aligned liquid crystal on silicon displays," Proc. SPIE 9216, 9216H (2014).
[29] F.J. Martínez, A. Márquez, S. Gallego, M. Ortuño, J. Francés, I. Pascual, and A. Beléndez, "Predictive capability of average Stokes polarimetry for simulation of phase multilevel elements onto LCoS devices," Appl. Opt. 54, 1379-1386 (2015).
[30] F.J. Martínez, R. Fernández, A. Márquez, S. Gallego, M. L. Álvarez, I. Pascual, and A. Beléndez. "Exploring binary and ternary modulations on a PA-LCoS device for holographic data storage in a PVA/AA photopolymer," Opt. Express 23, 20459-20479 (2015).
[31] A. Lizana, I. Moreno, A. Márquez, C. Iemmi, E. Fernández, J. Campos, and M. J. Yzuel, " Time fluctuations of the phase modulation in a liquid crystal on silicon display: characterization and effects in diffractive optics," Opt. Express 16, 16711-16722 (2008).
[32] G. Goldstein, [Polarized Light], Marcel Dekker (2003).
[33] F. J. Martínez, A. Márquez, S. Gallego, M. Ortuño, J. Francés, A. Beléndez, and I. Pascual, "Electrical dependencies of optical modulation capabilities in digitally addressed parallel aligned LCoS devices," Opt. Eng. 53, 067104 (2014).
[34] http://holoeye.com/spatial-light-modulators/gaea-4k-phase-only-spatial-light-modulator/ (visited on the 25th July 2017)
[35] J. Albero, P. García-Martínez, J. L. Martínez, I. Moreno, "Second order diffractive optical elements in a spatial light modulator with large phase dynamic range," Opt. Lasers Eng. 51, 111-115 (2013).
[36] A. Márquez, C. Iemmi, I. Moreno, J. Campos, and M. J. Yzuel, "Anamorphic and spatial frequency dependent phase modulation on liquid crystal displays. Optimization of the modulation diffraction efficiency," Opt. Express 13, 2111–2120 (2005).
[37] L. Lobato, A. Lizana, A. Márquez, I. Moreno, C. Iemmi, J. Campos and M. J. Yzuel, "Characterization of the anamorphic and spatial frequency dependent phenomenon in Liquid Crystal on Silicon displays," J. Eur. Opt. Soc. – Rapid Pub. 6, 11012S 1-6 (2011).